Available online at www.sciencedirect.com
SCIENCE DIRECT®
Journal of Power Sources 146 (2005) 658–663
JOURNAL OF POWER SOURCES
www.elsevier.com/locate/jpowsour

Electrochemical properties of $Li[Ni_xLi_{(1-2x)/3}Mn_{(2-x)/3}]O_2$ ($0 \leq x \leq 0.5$) cathode materials prepared by a sol–gel process

B.-J. Hwang *, C.-J. Wang, C.-H. Chen, Y.-W. Tsai, M. Venkateswarlu

Nanoelectrochem. Laboratory, Department of Chemical Engineering, National Taiwan University of Science and Technology, #43 Keelung Road, Section 4, Taipei 106, Taiwan

Available online 1 June 2005

Abstract

Layered $Li[Ni_xLi_{(1-2x)/3}Mn_{(2-x)/3}]O_2$ ($0 \leq x \leq 0.5$) cathode powders were synthesized by a sol–gel process. The synthesized $Li[Ni_xLi_{(1-2x)/3}Mn_{(2-x)/3}]O_2$ ($0 \leq x \leq 0.5$) powders were confirmed to be layered structure with a space group of $R\bar{3}m$ by X-ray diffraction (XRD) analysis. The extra diffraction peaks between 20° and 30° in the 2θ scale indicates the superlattice ordering of Li, Ni and Mn in the transition metal layer. Further, there is no change in the structural parameters up to $x = 0.2$, and thereafter, the changes are significant with increase of x value to 0.5. The surface morphology of the synthesized electrode powders was examined by scanning electron microscopy (SEM) and an average particle size was found to be in an order of 0.1–0.4 μm. The charge–discharge curves showed that the two distinguishable charge plateaus at the first cycle which were attributed to the Ni^{2+}/Ni^{4+} redox pair (≤4.5 V) and partial loss of oxygen (≥4.5 V), respectively. The stable discharge capacity of 260 mAh g^{-1} was obtained at the end of the 20th cycle for the $Li[Li_{0.2}Ni_{0.2}Mn_{0.6}]O_2$ electrode in the potential between 2.5 and 4.7 V at 12.6 mA g^{-1}. The electrode cell performance at $x = 0.2$ is the best among the studied x value in the $Li[Ni_xLi_{(1-2x)/3}Mn_{(2-x)/3}]O_2$ system.

Keywords: Sol–gel; XRD; SEM; Superlattice; Cathode; Cycle performance

1. Introduction

$Li[Li_{(1-2x)/3}Mn_{(2-x)/3}]O_2$ layer structure electrode materials were found to be an attractive cathode materials for an advanced lithium-ion batteries because of their high specific capacity and high potential plateau greater than at 4.5 V [1–5]. Recently, $Li[M_xLi_{(1-2x)/3}Mn_{(2-x)/3}]O_2$ (M = Co, Ni and Cr) cathode materials have been extensively investigated by partial substitution of $M = Ni^{2+}$ and Co^{3+}. Cr^{3+} for Li^+ and Mn^{4+} in the parent compound, $Li[Li_{1/3}Mn_{2/3}]O_2$, which will form a respective solid solutions between the $LiCoO_2$, $LiNiO_2$ and $LiCrO_2$, each with that of parent compound [4–10]. It is well known that the $Li[Li_{1/3}Mn_{2/3}]O_2$ electrode is electrochemically inactive because of existence of Mn as Mn^{4+} and further oxidation, i.e., beyond the Mn^{4+}, could not be possible [4]. The substitution of nickel in the $Li[Ni_xLi_{(1-2x)/3}Mn_{(2-x)/3}]O_2$ formula is of interest because it delivers large reversible capacity than its theoretical capacity. The substituted nickel (Ni^{2+}) can replace Li^+ and Mn^{4+} in the $Li[Li_{1/3}Mn_{2/3}]O_2$ electrode and form a complete solid solution of the $Li[Ni_xLi_{(1-2x)/3}Mn_{(2-x)/3}]O_2$ compound with layered characteristics [8].

Electrochemical properties of a series of $Li[Ni_xLi_{(1-2x)/3}Mn_{(2-x)/3}]O_2$, $Li[Cr_xLi_{(1-2x)/3}Mn_{(2-x)/3}]O_2$ and $Li[Co_xLi_{(1-2x)/3}Mn_{(2-x)/3}]O_2$ compounds were reported [4–13] and most of these electrodes delivered a large charge capacity. The observed specific capacity is larger than its theoretical capacity, especially, at the first cycle [4–13]. Dahn's group investigated the electrochemical and structural properties of this kind of materials extensively to understand the origin of the anomalous charge capacity at the first cycle. They proposed that the electrochemical phenomena that the charge capacity up to 4.3 V corresponds to the redox pair of Ni^{2+}/Ni^{4+} and an extra charge capacity drawn above 4.3 V plateau region was due to the extraction of lithium from lithium layer along with the simultaneous expulsion of oxygen for the charge compensation [8]. However, the weight loss measurements of

* Corresponding author. Tel.: +886 2 27376624; fax: +886 2 27376644.
E-mail address: bjh@ch.ntust.edu.tw (B.-J. Hwang).

0378-7753/$ – see front matter © 2005 Elsevier B.V. All rights reserved.
doi:10.1016/j.jpowsour.2005.03.090

a charged cathode could not provide any evidence about the evolution of oxygen during the first cycle [12]. On the other hand, Robertson and Bruce reported that a large irreversible capacity at the first cycle is due to exchange of Li^+ by H^+, H^+ is generated from an electrolyte, upon charging processes as evidenced from the nuclear magnetic resonance spectroscopy analysis [14]. The loss of oxygen and involvement of electrolyte in the electrochemical process will affect the capacity as well as cyclability of the electrode. Interestingly, this electrode material delivered a stable specific capacity for the subsequent cycles. Therefore, the understanding of electrochemical phenomena in this kind of electrode materials is of interest for both technological as well as scientific point of view. Thus, it is essential to investigate the $Li[Ni_xLi_{(1-2x)/3}Mn_{(2-x)/3}]O_2$ system for various nickel (x) content and the resulted electrochemical properties are useful for designing the electrode material for practical applications.

In this work, $Li[Ni_xLi_{(1-2x)/3}Mn_{(2-x)/3}]O_2$ $(0 \le x \le 0.5)$ electrode materials were synthesized by a sol–gel process and characterized by X-ray diffraction (XRD) and scanning electron microscopy (SEM). The electrode cell performance were tested in the potentials between 2.5 and 4.7 V with a specific charge and discharge currents at 12.6 mA g^{-1}. The electrochemical performance were evaluated for various x value in the $Li[Ni_xLi_{(1-2x)/3}Mn_{(2-x)/3}]O_2$ system and discussed by comparing with that of the $LiNi_{0.5}Mn_{0.5}O_2$ layered cathode.

2. Experimental

2.1. Preparation of the electrode powders

$Li[Ni_xLi_{(1-2x)/3}Mn_{(2-x)/3}]O_2$ $(0 \le x \le 0.5)$ powders were synthesized by a sol–gel process in which citric acid was used as a chelating agent. Stoichiometric amounts of lithium acetate, nickel acetate and manganese acetate were used as starting chemicals and dissolved in 100 mL of distilled water and stirred continuously. The solution temperature was raised to 80–90 °C and the solution was continued stirring for 5–6 h to form a high viscous gel. The gel was dried in a vacuum oven at 120 °C for 12 h. The precursor powder was decomposed at 450 °C for 4 h and naturally cooled to room temperature by turning furnace off [4,8]. The powder was made in the form of pellet and calcined at 900 °C for 12 h in air and quenched to room temperature (RT) by sandwiching the pellet between two copper plates.

2.2. Characterization by XRD and SEM

The synthesized $Li[Ni_xLi_{(1-2x)/3}Mn_{(2-x)/3}]O_2$ $(0 \le x \le 0.5)$ electrode powders were characterized by X-ray diffraction (Rikagu, XRD: Rotaflex) using Cu Kα radiation in the diffraction angle of 2θ range from 10° to 80° with a scan rate of 2°/min. The surface morphology and particle size distribution of the synthesized powders were examined using scanning electron microscopy (JEOL, JSM 6500). The samples were prepared by gold sputtering on the surface of the $Li[Ni_xLi_{(1-2x)/3}Mn_{(2-x)/3}]O_2$ $(0 \le x \le 0.5)$ powders. SEM images were taken at an accelerating voltage of 15 kV with a magnification 15,000×.

2.3. Electrode preparation and electrochemical measurements

The cathode film composed of $Li[Ni_xLi_{(1-2x)/3}Mn_{(2-x)/3}]O_2$ $(0 \le x \le 0.5)$ electrode powder as an active material, carbon black and KS6 graphite are as an conducting agents, and polyvinylidene fluoride (PVdF) as a binder, respectively, in the ratio of 85:3.5:1.5:10 (w/w). *N*-methyl pyrrolidinone (NMP) solvent was used as a dispersion medium. The resulting slurry was casted on the Al foil using a doctor blade. The coated Al foil was dried at 120 °C for 2 h to remove the NMP solvent. The Al foil was roll-pressed and punched into circular discs. The resulted electrode films were preserved in argon-filled dry box. The coin cell was assembled with $Li[Ni_xLi_{(1-2x)/3}Mn_{(2-x)/3}]O_2$ $(0 \le x \le 0.5)$ as a cathode, the lithium (FMC) metal foil as an anode and a mixture of equal volume of ethylene carbonate (EC):diethyl carbonate (DEC) (1:1) and $LiPF_6$ salt was used as an electrolyte. The polypropylene membrane (separator) was soaked in an electrolyte for 24 h prior to use. The coin cell was assembled in an argon-filled dry box (Unilab, Mbruan) in which the moisture and oxygen contents were maintained less than 1 ppm. Electrochemical studies were performed on a coin-type cell in the potential range of 2.5–4.7 V with a charge and discharge currents at 12.6 mA g^{-1} at room temperature.

3. Results and discussion

3.1. Structural parameters

X-ray diffraction patterns of various stoichiometry (x) in the $Li[Ni_xLi_{(1-2x)/3}Mn_{(2-x)/3}]O_2$ $(0 \le x \le 0.5)$ system are shown in Fig. 1. The XRD patterns of various x value in the $Li[Ni_xLi_{(1-2x)/3}Mn_{(2-x)/3}]O_2$ system were compared with that of the JCPDS pattern. The new diffraction peaks between 20° and 30° of 2θ scale in the XRD pattern indicates the superlattice ordering of Li, Ni and Mn in the transition metal layer. All other diffraction peaks were indexed based on the hexagonal structure, α-$NaFeO_2$ and a space group of $R\bar{3}m$. The well splitting of (1 0 8) and (1 1 0) peak intensity suggests that the synthesized powders are in good-layered characteristics. The lattice parameters (a and c) were calculated and the changes in the a, c and c/a ratio in the $Li[Ni_xLi_{(1-2x)/3}Mn_{(2-x)/3}]O_2$ $(0 \le x \le 0.5)$ system are shown in Fig. 2. It was found that the lattice parameters, a and c, does not change with x value up to 0.2 and then increases linearly with further increase of x value. In contrast to that the c/a ratio, changes are insignificant up to $x = 0.2$ and thereafter decreases with increase of x value in the $Li[Ni_xLi_{(1-2x)/3}Mn_{(2-x)/3}]O_2$.

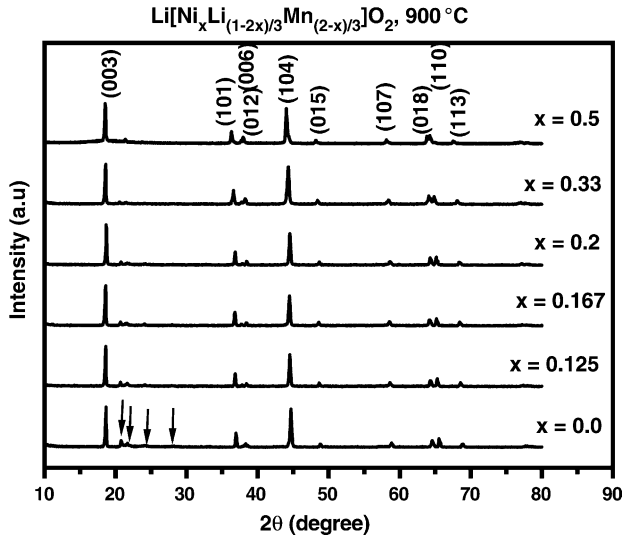

Fig. 1. XRD patterns for various x in $Li[Ni_xLi_{(1-2x)/3}Mn_{(2-x)/3}]O_2$.

The appearance of extra diffraction peaks so called "the superlattice reflections" were observed up to $x = 0.2$ and thereafter less pronounced with increase of x value up to 0.5. It indicates that the electrode symmetry reduced from $R\bar{3}m$ (hexagonal) to the $C2/m$ (monoclinic) with decrease of x value in the $Li[Ni_xLi_{(1-2x)/3}Mn_{(2-x)/3}]O_2$ system.

3.2. Surface morphology

The surface morphology of the $Li[Ni_xLi_{(1-2x)/3}Mn_{(2-x)/3}]O_2$ ($0 \le x \le 0.5$) powders for $x = 0.125$, 0.2 and 0.5 are shown in Fig. 3. From Fig. 3a–c, it can be seen that the crystal faces are well defined and the distribution of particles are non-uniform. Further, the particle size increases with increase of x value and partial agglomeration of these particles, especially at low x value were observed. The average diameter of the particles were found to be in the order of 0.2–0.3 μm for $x = 0.125$ and 0.1–0.2 μm for $x = 0.2$. The particle size slightly increases with increase of x value. The well-developed crystalline particles with regular shape and morphology were observed for $x = 0.5$ and an average diameter of these particles were found to be in the order of 0.2–0.3 μm. Earlier, it has been demonstrated that the good crystalline particles and uni-

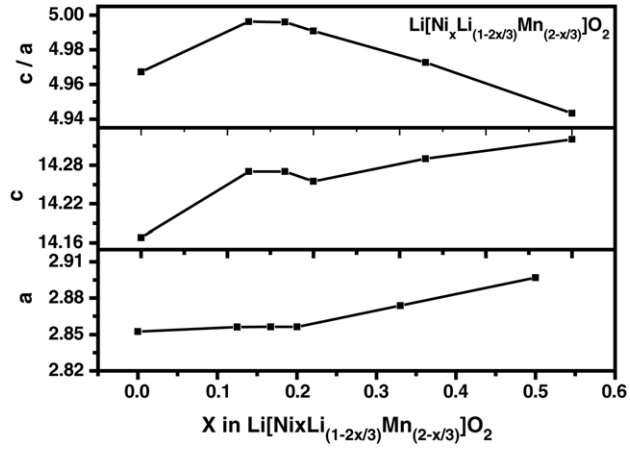

Fig. 2. Lattice parameter variation with x in $Li[Ni_xLi_{(1-2x)/3}Mn_{(2-x)/3}]O_2$.

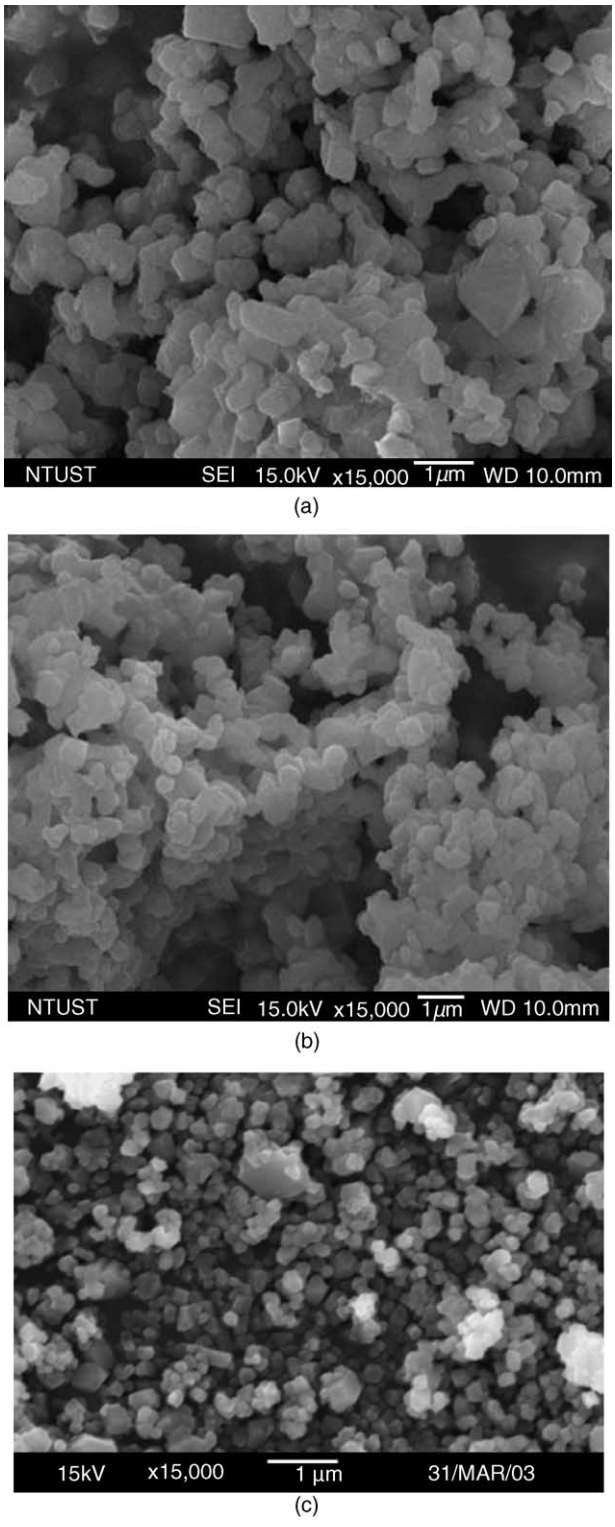

Fig. 3. SEM micrographs for (a) $x = 0.125$, (b) $x = 0.2$ and (c) $x = 0.5$ in $Li[Ni_xLi_{(1-2x)/3}Mn_{(2-x)/3}]O_2$.

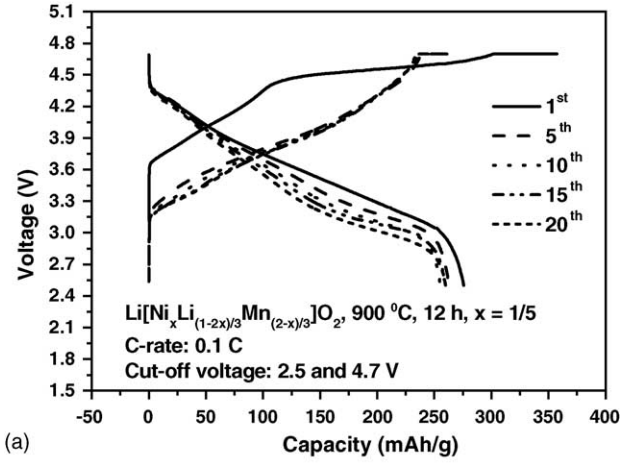

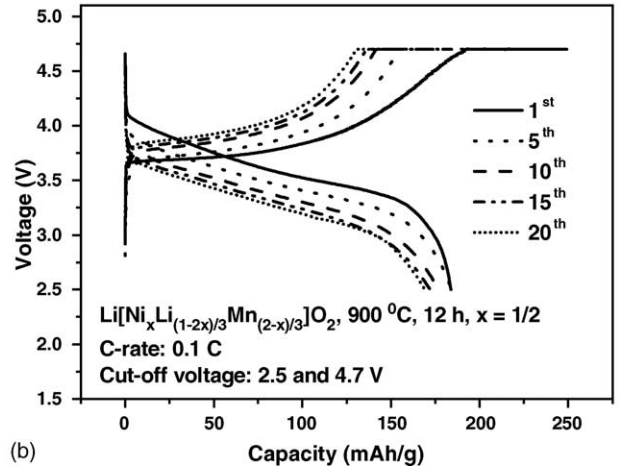

Fig. 4. (a) Voltage profile for $x = 0.2$ in $Li[Ni_xLi_{(1-2x)/3}Mn_{(2-x)/3}]O_2$ and (b) voltage profile for $x = 0.5$ in $Li[Ni_xLi_{(1-2x)/3}Mn_{(2-x)/3}]O_2$.

form particle size distribution (PSD) will improve the electrochemical performance of the synthesized electrode powders [15,16]. However, the crystallinity, particle size and PSD of the synthesized powders change insignificantly with the stoichiometry of nickel (x) in the $Li[Ni_xLi_{(1-2x)/3}Mn_{(2-x)/3}]O_2$ system, indicating that they are not the key factors responsible for the significant variation of the electrochemical performance of the synthesized powders at various compositions.

3.3. Electrochemical properties

Fig. 4a and b shows the voltage profile for $x = 0.2$ and 0. 5, respectively, for the $Li[Ni_xLi_{(1-2x)/3}Mn_{(2-x)/3}]O_2$ electrode cycled at 12.6 mA g^{-1} in the potential range of 2.5–4.7 V. The potential difference between the charge and discharge curves is large at the first cycle due to the increase of internal resistance and gradually decreases for the subsequent cycles. The best charge and discharge capacities of 357 and 275.8 mAh g^{-1} at the first cycle and the specific charge and discharge capacity of each at 260 mAh g^{-1} was obtained at the end of the 20th cycle for $x = 0.2$ (Fig. 4a). The irreversible capacity was found to be 81.2 mAh g^{-1}, is around 23% of its first charge capacity, and for the subsequent cycles, the irreversible capacity decreases significantly with increase of cycle number. The columbic efficiency was found to be almost 100% at the end of 20th cycle and the smooth charge and discharge curves suggest that the electrode stability upon the lithium intercalation and de-intercalation during cycling processes. The charge and discharge capacities were found to be 249 and 183 at the first cycle and 174.6 and 169 mAh g^{-1}, respectively, at the end of the 20th cycle for $x = 5$ (Fig. 4b). The electrochemical cell performance of $x = 0.2$ is superior among the studied x values in the $Li[Ni_xLi_{(1-2x)/3}Mn_{(2-x)/3}]O_2$ ($0 \le x \le 0.5$) in the potential range 2.5–4.7 V. It suggests that the electrodes having superlattice ordering could deliver a higher specific capacity than that of the layered characteristics electrode, however further studies are required to confirm it. The cyclability of the $Li[Ni_xLi_{(1-2x)/3}Mn_{(2-x)/3}]O_2$ electrodes for various x value are shown in Fig. 5 and the x values at 0 and 0.5 are also included in Fig. 5 for comparison. It can be noticed that the capacity retention was good for $x = 0.2$, which consists of extra diffraction lines as evidenced from XRD pattern (Fig. 1). The specific capacity of 260 mAh g^{-1} with better capacity retention (4.4%) was obtained for the $Li[Ni_{0.2}Li_{0.2}Mn_{0.4}]O_2$ electrode after 20th cycle. The electrochemical performance of the $Li[Ni_{0.2}Li_{0.2}Mn_{0.4}]O_2$ electrode prepared by different methods are presented in Table 1. It can bee seen from Table 1 that the electrode materials synthesized by a sol–gel process delivered a better specific capacity with better capacity retention in the potential range 2.5–4.7 V. It is probably that the sol–gel process developed in this work is capable of providing the cathode powders with better crystallinity and morphology compared to the other methods.

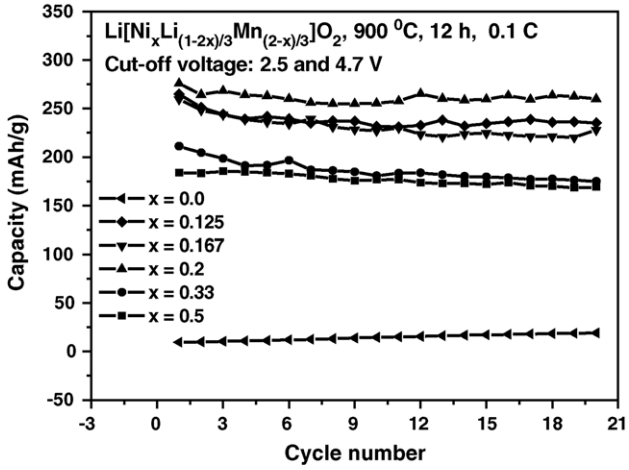

Fig. 5. Cyclability for various x in $Li[Ni_xLi_{(1-2x)/3}Mn_{(2-x)/3}]O_2$.

In order to understand the origin of 4.5 V charge plateau at the first cycle, Dahn and co-workers proposed the electrochemical mechanism by splitting the first charge plateau region into two well defined regions such as below to the 4.3 V and above to the 4.3 V. The first charge plateau region (<4.3 V) was attributed to redox pair of Ni (Ni^{2+}/Ni^{4+})

Table 1
Comparison of the electrochemical performance of the $Li[Ni_{0.2}\ Li_{0.2}\ Mn_{0.4}]O_2$ electrode

Preparation methods	Initial charge capacity ($mAh\,g^{-1}$)	Initial discharge capacity ($mAh\,g^{-1}$)	Discharge capacity and capacity retention for 20 cycles	Reference
Sol–gel	240	155 at 10 mA g^{-1} (2.0–4.6 V)	205 mAh g^{-1}, good	[11]
Combustion	≈322	288 at 20 mA g^{-1} (2.0–4.8 V)	221 mAh g^{-1}, 76.7%	[12]
Sol–gel	≈350	268 at 0.1mA/cm^2 (2.5–4.6 V)	212 mAh g^{-1}, 79.1%	[13][a]
Sol–gel	357	275.8 at 12.6 mA g^{-1} (2.5–4.7 V)	260 mAh g^{-1}, 94.3%	Present work

[a] 0.2 and 0.4 mA cm^{-2} were used for 2 and 3 to 20 cycles, respectively.

and the second charge plateau was ascribed to an extraction lithium from the lithium layer with the simultaneous expulsion of oxygen in order to compensate the charge balance and to maintain the charge neutrality in the $Li[Ni_xLi_{(1-2x)/3}Mn_{(2-x)/3}]O_2$ system [7–12]. Recently, Hong et al. did not find any evidence for the expulsion of oxygen while extraction of lithium-ions at the first cycle based on the weight loss measurements of the charged cathode. But, they confirmed that the loss of oxygen occurred between the $0.4 \le y \le 1.0$ range in the $Li_{1-y}[Ni_{0.2}Li_{0.2}Mn_{0.6}]O_2$ [12]. In recent NMR spectroscopic analysis revealed that the excess charge capacity and a large irreversible capacity at the first cycle was due the exchange of Li^+ by H^+ during charging process [14]. However, the electrochemical phenomena at the first charge plateau and its contributing factors and the corresponding capacity loss are still remain as mystery in the $Li[Ni_xLi_{(1-2x)/3}Mn_{(2-x)/3}]O_2$ electrode system.

From Fig. 5, it can be noticed that the discharge capacity is stable with increase of cycle number and the columbic efficiency was found to be almost 100% at the end of the 20th cycle. Kang et al. speculated that the stable capacity was due to the removal of lithium-ions from the transition metal layer [11], which has also been confirmed by NMR [17]. The stable capacity with better retention of the studied electrode materials suggests that Mn stabilizes the electrode structure due to its existence as Mn^{4+} and Mn^{3+}, respectively, at the end of the charging and discharging during cycling processes [18]. We speculate that the cation ordering in the transition metal layer play a crucial role in stabilizing the electrode structure as a result of the improvement of its capacity. Further, the stability of the electrode depends on the existence of cation ordering in the transition metal layer and these concluding remarks are consistent with that of the recent reported results based on the nuclear magnetic spectroscopy (NMR) and the first principle calculations by Yoon et al. [17,19]. In order to verify the electrochemical charge and discharge phenomena in an elucidate manner, we have performed X-ray absorption spectroscopy (XAS) investigations to understand the local environment of the prepared electrode materials and results are under process to communicate shortly.

4. Conclusions

Novel $Li[Ni_xLi_{(1-2x)/3}Mn_{(2-x)/3}]O_2$ ($0 \le x \le 0.5$) cathode materials were successfully synthesized by a sol–gel process. The synthesized powders with high phase purity and layered structure were confirmed by the X-ray diffraction analysis. The new diffraction peaks between 20° and 30° of 2θ in the XRD pattern was attributed to the superlattice ordering of Li, Ni and Mn in the transition metal layer. The crystallinity, particle size and PSD of the synthesized powders are similar, indicating that they are not the key factors responsible for the significant variation of their electrochemical performance at various compositions. The first cycle charge curve showed the two distinguishable potential plateaus and the correspondingly charge plateaus are due to the redox pair of Ni^{2+}/Ni^{4+} and partial oxygen loss, respectively. The stable specific capacity of 260 mAh g^{-1} with better capacity retention was obtained for the $Li[Ni_{0.2}Li_{0.2}Mn_{0.4}]O_2$ electrode in the potentials between 2.5 and 4.7 V at 12.6 mA g^{-1}. The electrochemical cell performance of these electrodes suggests that these prepared electrodes can be used as a cathode for advanced lithium-ion batteries.

Acknowledgements

The support from the National Science Council (NSC-93-ET-7-011-002-ET), the Ministry of Education of Taiwan (EX-93-E-FA09-5-4) and National Taiwan University of Science and Technology is acknowledged.

References

[1] H. Arai, S. Okada, Y. Sakurai, J.I. Yamaki, J. Electrochem. Soc. 144 (1997) 3117.
[2] T. Ohzuku, Y. Makimura, Chem. Lett. (2001) 744.
[3] B.J. Hwang, Y.W. Tsai, D. Carlier, G. Ceder, Chem. Mater. 15 (2003) 3676.
[4] Z. Lu, D.D. MacNeil, J.R. Dahn, Electrochem. Solid State Lett. 4 (2001) A191.
[5] Z. Lu, J.R. Dahn, J. Electrochem. Soc. 149 (2002) A1454.
[6] Z. Lu, R.A. Donaberger, J.R. Dahn, Chem. Mater. 12 (2000) 3583.
[7] Z. Lu, L.Y. Beaulieu, R.A. Donaberger, C.L. Thomas, J.R. Dahn, J. Electrochem. Soc. 149 (2002) A778.
[8] Z. Lu, J.R. Dahn, J. Electrochem. Soc. 149 (2002) A815.
[9] D.D. MacNeil, Z. Lu, J.R. Dahn, J. Electrochem. Soc. 149 (2002) A1332.
[10] Y.J. Park, Y.S. Hong, X. Wu, M.G. Kim, K.S. Ryu, S.H. Chang, J. Electrochem. Soc. 151 (2004) A720.
[11] S.H. Kang, Y.K. Sun, K. Amine, Electrochem. Solid State Lett. 6 (2003) A183.

[12] Y.S. Hong, Y.J. Park, K.S. Ryu, S.H. Chang, M.G. Kim, J. Mater. Chem. 14 (2004) 1424.
[13] J.H. Kim, Y.K. Sun, J. Power Sources 119–121 (2003) 166.
[14] A.D. Robertson, P.G. Bruce, Chem. Mater. 15 (2003) 1984.
[15] V. Manev, W. Ebner, W. Thompson, S. Dow, US Patent 5,961,949 (1999).
[16] B.J. Hwang, Y.W. Tsai, C.H. Chen, R. Santhanam, J. Mater. Chem. 13 (2003) 1962.
[17] W.S. Yoon, N. Kim, X.Q. Yang, J. McBreen, C.P. Grey, J. Power Sources 119–121 (2003) 649.
[18] J. Reed, G. Ceder, Electrochem. Solid State Lett. 5 (2002) A145.
[19] W.S. Yoon, S. Iannopollo, C.P. Grey, D. Carlier, J. Gorman, J. Reed, G. Ceder, Electrochem. Solid State Lett. 7 (2004) A167.